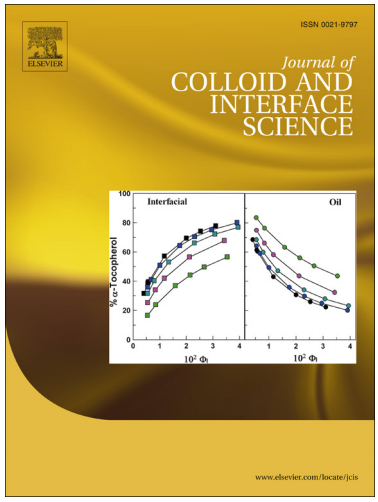

Effect of the morphology of synthetic kaolinites on their sorption properties

Lei Lei Aung, Emmanuel Tertre, Sabine Petit

PII: S0021-9797(14)00952-7
DOI: http://dx.doi.org/10.1016/j.jcis.2014.12.008
Reference: YJCIS 20051

To appear in: *Journal of Colloid and Interface Science*

Received Date: 7 July 2014
Accepted Date: 2 December 2014

Please cite this article as: L.L. Aung, E. Tertre, S. Petit, Effect of the morphology of synthetic kaolinites on their sorption properties, *Journal of Colloid and Interface Science* (2014), doi: http://dx.doi.org/10.1016/j.jcis.2014.12.008

Effect of the morphology of synthetic kaolinites on their sorption properties

Lei Lei Aung[a,b] , Emmanuel Tertre[a,*] , Sabine Petit[a]

[a]Université de Poitiers-CNRS, UMR 7285 IC2MP, Equipe HydrASA, rue Albert Turpain, Bat. B8, 86022 Poitiers Cedex, France.

[b]Division of Biotechnology, School of Bioresources and Technology, King Mongkut's University of Technology Thonburi, Bangkok 10150, Thailand.

*Corresponding author: Tel: (00) 33 5 49 45 36 57

E-mail: emmanuel.tertre@univ-poitiers.fr

Abstract

Natural kaolinites often have a permanent charge due to mineralogical impurities preventing to link directly the morphology of the kaolinite particle to a selectivity coefficient between two cations for edge sites. In this study, kaolinites with no permanent charge were hydrothermally synthesized under different physicochemical conditions to obtain various morphologies (hexagon-shaped, more or less anisotropic). Na^+ and H^+ were chosen as the sorbed cations due to their ubiquitous presence in natural waters. For synthetic kaolinites for which no swelling layer was detected, an experimental sorption isotherm between Na^+ and H^+ was obtained. Data were interpreted using a surface complexation model, containing no electrostatic term, by considering the specific surfaces of lateral sites and sorption site density identified by crystallography for the different faces presented in the samples ((010), (110), (1-10)). Selectivity coefficients between Na^+ and H^+ for all lateral sites characterizing a given morphology were calculated and validated in the [4-10] pH range, corresponding to the pH range for which dissolution can be considered negligible. The results showed that the Na^+/H^+ selectivity coefficient depends strongly on the particle morphology and that the sorption properties of kaolinites cannot be obtained with good accuracy without a fine knowledge of the morphology of the particles.

Keywords: Kaolinite/Morphology/Selectivity coefficient/Na-H sorption isotherm

1. Introduction

Kaolinite is a 1:1-type aluminosilicate clay [$(Si_4)^{IV}(Al_4)^{VI}O_{10}(OH)_8$] in which one tetrahedral sheet is combined with one octahedral sheet, forming a layer stack. Octahedral and tetrahedral sheets are linked to each other by common oxygen atoms, whereas adjacent layers are bound together by hydrogen bonds (Brigatti et al., 2006). This structure results in a crystal that presents different surfaces to its environment: a siloxane face (basal surface), an alumina face with $>Al_2OH$ groups (basal surface) and lateral surfaces with silanol (>SiOH) and aluminol (>AlOH) groups. As oxides and hydroxides, pure kaolinite is characterized by a surface charge that solely on the pH, which is due to the protonation and deprotonation of hydroxyl groups (>SiOH and >AlOH) located on the edges of the particles (Johnston and Tombácz (2002); Wypych and Satyanarayana (2004), among others). The reactivity of the aluminol groups located on the alumina face ($>Al_2OH$) is generally considered negligible in the pH range in which sorption studies are generally performed (pH from 2 to 10)) (see discussions in Huertas et al. (1998) and Tertre et al. (2006a)). Depending on the aqueous pH, the surface charges enhance or inhibit metal sorption (Bhattacharyya and Gupta, 2008), and cation sorption is associated with the release of hydrogen ions (H^+) from the edge sites (Gu and Evans, 2008).

Many studies devoted to the sorption of inorganic cations on kaolinites, suspended in aqueous solutions, have been conducted (Miranda-Trevino and Coles, 2003; Tertre et al., 2006a; Gu and Evans, 2008, among others). These studies have been motivated by the ubiquity of this mineral in many natural geological environments (soils, sediments, natural water). Furthermore, the monovalent cation sodium is one of the major ions in natural waters (from ~10^{-3} to ~0.5 mol/L in rivers and seas, respectively) and can also be found in relatively high concentrations in the surface waters of growing urban areas (Buttle and Labadia, 1999). In this context, the sodium cation is found in effluents from industrial and municipal

facilities, and its presence in natural waters at irregular levels adversely affects the municipal and private water supplies (Cleary, 1978), soil chemistry and the aquatic environment. In this context, it is crucial to have tools such as a selectivity coefficient to predict the ion-exchange of this cation on kaolinites with good confidence, particularly with respect to the H^+ that is always present and reactive in natural and artificial waters. Finally, the sorption properties of Na^+ toward clay surfaces is also crucial to be well predicted because trace metallic cations are always in competition with this major cation for sorption on solid surfaces in natural environments (see discussion in Tertre et al., 2011 for example).

In the literature, the effect of particles' morphology on their sorption properties has been studied for oxides and hydroxides (Bi et al., 2010; Zhang et al., 2010, among others). However, as far as the authors are aware, the influence of the morphology of kaolinite particles on their sorption properties has not been studied to date because, generally in experimental studies, (1) the samples used contain mineralogical and/or organic impurities that are responsible for the presence of a permanent charge, and (2) the chemistry of the aqueous phase is not fully controlled. For example, even the low-defect Georgia kaolinite commercialized by the Clay Mineralogical Society (KGa--1b) has a low permanent charge of 0.6 meq/100 g (Schroth and Sposito, 1997; Wan and Tokunaga, 2002), most likely due to the presence of a few organic impurities or swelling layers. Because natural materials rich in kaolinite very often contain traces of swelling layers (Ma and Eggleton, 1999) that are responsible for a significant permanent charge on the whole material, a synthetic approach was used in this study to obtain kaolinites with zero permanent charge that differed by their size and/or morphology. Fialips et al. (2000) showed that it is possible to synthesize different kaolinites distinguished by their crystallinity and morphology (from hexagonal to lath-shaped particles), all characterized by zero permanent charge, by applying hydrothermal synthesis to a partially crystallized gel and using different pH values for synthesis.

The first aim of this study is to obtain synthetic kaolinites according to the hydrothermal procedure proposed by Fialips et al. (2000) and to characterize the synthetic products in terms of mineralogy, crystal chemistry, cation exchange capacity and size/morphology of the particles. Then, for synthetic products for which cation exchange capacity can be attributed to the sole kaolinite phase, the experimental sorption isotherms between Na^+ and H^+ are obtained and interpreted according to a surface complexation model containing no electrostatic term. This latter procedure, associated with knowledge of the morphology of the synthetic products and the sorption site densities of the main faces ((010), (110), (0-10)) presented in our samples, allows us to propose a selectivity coefficient between Na^+ and H^+ for the whole of the lateral sites characterizing a given particle morphology. The edge site density fraction involved in the dissolution process, a process that cannot be totally avoided when Na^+ sorption is studied as a function of pH, is discussed and allows us to assess the pH range for which the selectivity coefficient we propose is valid.

2. Materials and methods

2.1. Materials

Kaolinites were hydrothermally synthesized from amorphous silicoaluminous gel, as described in detail in Fialips et al. (2000). Briefly, the amorphous gel was obtained by mixing 1 M sodium metasilicate solution (prepared from dissolution of the $SiO_2Na_2O{\cdot}5H_2O$ salt) with 1 M aluminum nitrate solution (prepared from dissolution of the $Al(NO_3)_3{\cdot}9H_2O$ salt) and 1 M sodium hydroxide solution (NaOH), according to the stoichiometry of the following reaction:

$$2SiO_2Na_2O + 2Al(NO_3)_3 + 2NaOH \longrightarrow 6NaNO_3 + H_2O + Si_2Al_2O_7 \qquad \text{Reaction 1}$$

The resulting gel ($Si_2Al_2O_7$) was washed several times with pure water to remove the sodium nitrate salt, dried in an oven at 60°C overnight, and ground to powder in an agate

mortar. The amorphous character of the gel was checked by X-ray diffraction (XRD) analysis (see Figure S.I.1 in Supporting Information). Then, the gel (500 mg) was mixed with 30 mL of distilled water in a Teflon® reactor. The initial pH of this mixture was approximately 5. The mixture was heated in an oven at 220°C under equilibrium water pressure (23.2 bar) over 14 days. At the end of this step, the gel was transformed into partially crystallized kaolinite and regarded as Starting Material (SM).

The SM was mixed with distilled water using a solid/water ratio equal to ~13 g/L. Hydrothermal synthesis was conducted for ten different initial pH values (pH_I), equal to approximately 1.0, 1.2, 5.0, 5.1, 8.1, 8.3, 10.8, 10.9, 11.2 and 11.4, and adjusted by the addition of small quantities of 1 M HCl and 1 M NaOH solutions at room temperature. Initial pH values were chosen according to the results of Fialips et al. (2000) to obtain contrasted morphologies for the different synthesized kaolinites. Hydrothermal syntheses were performed in an oven at 240°C for 21 days. Finally, the pH (pH_F) of the clay suspension was measured at the end of the synthesis at 25°C. Then, the synthesized kaolinites were dried in an oven at 60°C overnight, ground to powder and Na-saturated. This last step was performed to ensure that all sorption sites located on the surfaces of the synthetic particles were fully saturated with only one type of cation (Na^+ in our case). The saturation procedure and the steps to remove excess chloride used in this study were described by Tertre et al. (2013). After these steps, each rinsed sample was dried in an oven at 60°C overnight and gently crushed. The final synthetic products are referred as $pH_F = 0.8$ to $pH_F = 8.3$, according to the final pH of their synthesis.

2.2. Methods

2.2.1. Methods for solid characterization

X-Ray Diffraction (XRD). For each synthetic kaolinite, XRD powder patterns were recorded in the 5° to 65° 2θ CuKα angular range with a 0.025 degree step, using an acquisition time of 1.2 s per step on a Bruker® D8 advanced diffractometer equipped with Ni-filtered CuKα radiation (1.5418 Å) generated at 40 kV and 40 mA. In addition, the XRD patterns of oriented preparations of some synthetic samples were registered to investigate the possible presence of swelling minerals in the samples. These acquisitions were performed under both air dried and ethylene glycol conditions. For these oriented samples, XRD patterns were recorded in the 5° to 50° 2θ range with a 0.025 degree step and using an acquisition time of 1 s per step.

Defects in the kaolinite were characterized by the Hinckley Index (HI) corresponding to the ratio between (1) the sum of the heights of the d_{001} and d_{111} measured from the inter-peak background, and (2) the height of the d_{110} peak from the background. This index is sensitive to all crystalline defects (i.e., ±nb/3 translations, ±nπ/3 rotations, and random defects). Higher is the index value, lower is the defect density (Hinckley, 1963). Furthermore, the structural order obtained with the R_2 index proposed by Liétard (Liétard, 1977; Cases et al., 1982) was calculated from the intensities of the d_{131} and d_{131} reflections. This parameter is relative to the triclinic character of the crystals. Using the Sherrer formula (Langford and Wilson, 1978; Brindley and Brown, 1980), the crystal sizes of the coherent domain (CSD) were estimated from the d_{001} reflection (CSD_{001}) and the d_{060} reflection (CSD_{060}) along the c* axis and b axis, respectively.

Fourier-Transform Infrared Spectroscopy (FTIR). Fourier-Transform Infrared (FTIR) Spectra were obtained in the transmission mode at a resolution of 4 cm^{-1} in the mid-IR range

(4000-400 cm^{-1}) on a Nicolet® 760 FTIR spectrometer. Samples were prepared using the KBr method. The sample (1 mg) was mixed thoroughly with 100 mg of ground potassium bromide (KBr), and the mixture was pressed into pellets that were heated in an oven at 110°C overnight. The integrated intensity of the absorption bands was measured by using the OMNIC® software.

Transmission Electron Microscopy (TEM). Morphological study of the synthetic particles was carried out by TEM with a JEOL® Electron Microscope JEM1010, using 80 kV for the accelerating voltage. The sample was dispersed in distilled water at a ratio of 1:100 by ultrasonic probe, and a drop of the clay suspension was placed on a Ni-coated microgrid holder and air-dried at room temperature before the analysis.

Cation Exchange Capacity (CEC). For each Na-saturated synthetic kaolinite, CEC was measured. For that measurement, sorbed Na^+ was displaced with Cs^+ at pH = 9 by mixing 50 mg of Na-saturated kaolinite with 5 mL of a 1 M CsCl solution, and the pH was adjusted by the addition of small quantities of a 10^{-2} M CsOH solution. After mechanical shaking for 4 days, a clear supernatant was obtained from the centrifugation of the clay suspension. Then, the CEC of the sample was calculated from analysis of the Na^+ concentration measured in the supernatant using Atomic Absorption Spectroscopy (AAS).

Brunauer-Emmet-Teller (BET) method. A Micromeritics® ASAP 2000 was used to determine the specific surface area (SSA) of some samples. The measurements were performed at a batch temperature of 77.3 K and a relative pressure (P/P0) ranging up to 1. Prior to analysis, the samples were degassed with nitrogen gas at 350°C for 4 hours. The

specific surface area, corresponding to the specific surfaces of both basal and lateral surfaces, was calculated using the Brunauer-Emmet-Teller method (Brunauer et al., 1938).

***Method used to assess specific surface of edges*.** To assess the specific surface of the edges (specific lateral surface), TEM images and XRD data were used. From TEM images of 20 particles per sample, an average value of the perimeter of the basal surface of the particles was assessed. For this assessment, a perfectly monodisperse regular hexagonal arrangement was assumed, as performed by Hassan et al. (2005) for pseudo-hexagonal particles, while only the contribution of the (010) face was taken into account for lath-shaped particles. Then, we assumed that the average thickness of one particle could be assessed from XRD data considering the Scherrer Equation (Brindley and Brown, 1980), given the size of the coherent domain along the c axis. With both the average perimeter of the basal surface obtained with TEM and the average thickness obtained as described above, an average value for the lateral surface (edge surface) was estimated. These data allowed us also to calculate the average volume of the particle. By assuming a grain dry density equal to 2.62 (Ma and Eggleton, 1999), the specific lateral surface was assessed. To validate such an approach, the sum of both specific lateral and basal surfaces obtained by considering these geometric considerations will be compared with the measured BET surface. Finally, although absolute geometrical surfaces obtained from analyses of MET images can be overestimated because larger particles can be analyzed more than smaller particles, normalization to the mass of the particle avoids overestimation of the specific lateral and basal surfaces.

2.2.2. Na^+/H^+ sorption isotherms

Na^+/H^+ sorption isotherms were obtained for synthetic kaolinites for which the presence of a permanent charge and a swelling phase were not detected. The Na^+/H^+ sorption

isotherms were performed at an equilibrium pH ranging from 4 to 11. The protocol used in this study is fully detailed in Tertre et al. (2013). Some steps of the procedure are as follows: 40 mg of Na-saturated dried kaolinite was equilibrated for 3 days under agitation with 5 mL of an aqueous solution containing 0.25 M NaCl and characterized by a given pH value fixed by addition of small aliquot (50 µL maximum) of a 10^{-2} M NaOH or HCl solution, depending on the pH investigated. By doing that, total normalities in chloride of the solutions were equal to about 2.5×10^{-1} mol/L with a maximum variation of 5% between the different samples. After centrifugation, the pH values of the supernatants were measured, as well as their aqueous Na^+ concentrations at equilibrium. Then, sodium sorbed onto the kaolinite surfaces was desorbed by using a 1 M ammonium acetate solution under mechanical shaking for 2 days. The mixture was centrifuged again, and the concentration of aqueous Na^+ in the supernatant was measured. The formula used to determine the quantity of Na^+ sorbed onto the solid sample from these measurements can be found in Tertre et al. (2011).

2.2.3 Methods for aqueous analysis

pH. The pH value of the aqueous solutions was measured with a combined Metrohm® electrode calibrated with 3 NIST pH buffer solutions at 25°C. The uncertainty in the measured pH was estimated to be ± 0.05 pH unit.

Aqueous Na^+ concentrations. The concentrations of aqueous Na^+ were measured using an atomic absorption spectrophotometer (Varian® AA240FS). Before the analyses, aqueous samples were prepared in 2% HNO_3 solution, and 1 M ammonium acetate solution was added to the Na standards used to measure samples rich in ammonium to account for possible

interference during acquisition. The aqueous detection limits were 0.2 mg/L, and the total uncertainty in the measured concentration of Na^+ was estimated to be ±2%.

Aqueous silica content. The concentrations of aqueous silica were measured in each supernatant to assess the proportion of the edges dissolved along the Na^+/H^+ isotherms. These measurements were obtained according to the molybdate blue method (Strickland and Parsons, 1972) using a JENWAY® 6300 spectrophotometer at a wavelength of 820 nm. Detection limit was 0.5 mg/L and uncertainty of ± 5% may be assessed based on reproducibility tests. From these measurements, the percentages of the edge sites involved in the dissolution processes were calculated. For that calculation, the specific surfaces assessed for lateral sites obtained from morphology particles and the theoretical site density of kaolinite equal to 20 sites/nm^2 (Koretsky et al., 1998) were used. We assume that the uncertainty on the proportion of edges dissolved during experiments is due only to uncertainty of the concentration of aqueous silica measured (i.e., ±5%).

3. Results and discussion

3.1. Characterization of the synthetic kaolinites

3.1.1. X-ray diffraction analysis

XRD powder patterns of the starting material and synthetic kaolinites are shown in Figure 1. For samples prepared under acidic conditions ($0.8 \leq pH_F \leq 5.1$), narrow and intense peaks corresponding to the d_{001} and d_{020} reflections (~7.16 Å and ~3.57 Å, respectively) of kaolinites are observed (Figure 1), suggesting that these kaolinites are well-crystallized and contain low defect densities. These peaks become weak and broad with increasing pH_F. For $pH_F \geq 7.4$, less crystallization occurs. Small amounts of pseudoboehmite are also revealed over the entire pH_F range. Pseudo-boehmite peaks are identified at around 6.3 and 3.2 Å for

samples synthesized under both acidic and basic conditions (from pH_F = 0.8 to 8.3) and a supplementary broad peak occurring at 10-15 Å for the samples synthesized under the most basic conditions (pH_F = 7.9 and 8.3) (see Figure 1). Boehmite is a chemical precursor of kaolinite (Tsuzuki, 1976; Satokawa et al., 1994), and the presence of pseudoboehmite in our samples allows to form kaolinite, as previously detailed by Fialips et al. (2000).

A generally positive relationship between synthetic pH_F and the amount of defects is observed (Figures S.I.2A and B in Supporting Information). Indeed, the HI value is nearly constant for samples synthesized at an acidic pH ($0.8<pH_F<5.1$), and the HI value decreases for $pH_F>5.1$. For synthesis experiments, Miyawaki et al. (1991) and Fialips et al. (2000) reported that HI is directly proportional to the kaolinite yield. The percent crystallization of SM into well-ordered kaolinite in our synthetic products is higher when the final pH of crystallization is acidic than when it is basic. The R_2 parameter decreases with an increase in the final pH of synthesis (Figure S.I.2B), revealing that samples synthesized under basic conditions have a more monoclinic character than samples obtained under acid conditions.

The pH of the synthesis (pH_F) also has a strong effect on the apparent CSDs both along the c* and the b axis (Figures 2A and 2B, respectively). The effect is globally stronger along the c*axis. However, for pH values up to 5, the CSD_{001}—which can be considered the particle thickness—does not vary, as reported by Fialips et al. (2000).

.

3.1.2. Fourier Transform Infrared Spectroscopy (FTIR)

The FTIR spectra of kaolinites synthesized at different final pH values are shown in Figure 3. For most of the samples, the four typical hydroxyl bands of kaolinite can be observed at 3693, 3668, 3651 and 3620 cm^{-1} (Farmer, 1974; Madejova et al., 2011). Bands are more intense and well-resolved for samples prepared under acidic conditions ($0.8<pH_F<5.1$), suggesting that these samples are well-ordered (Fialips et al., 2000). In

contrast, peak intensities decrease, and the 3668 and 3651 cm^{-1} bands merge into a broad band for samples prepared at higher pH_F. Concomitantly, a shoulder appears at approximately 3600 cm^{-1}. A shoulder at 3600 cm^{-1} is commonly observed for iron-rich kaolinite and is due to Al-Fe^{3+}-OH vibrations (Petit et al., 1990; Iriarte et al., 2005). However, the band observed here cannot be attributed to such vibrations because there is no iron in the samples. Dudkin et al. (2005) described the appearance of a broad low intensity peak at 3610 cm^{-1} arising from molecular water upon grinding of natural kaolinite due to the disordered structure of the surface and internal OH groups. As all of our samples are gently ground, the 3600 cm^{-1} shoulder we observed could be due to the intrinsic disorderly nature of the kaolinite synthesized at pH_F>5. In the 400-1400 cm^{-1} range, the observed bands correspond to kaolinite (Farmer, 1974), and no other compound can be observed except for the SM, in which part of the unreacted product and boehmite are identified by a band at approximately 500 cm^{-1} (Fialips et al, 2000).

3.1.3. Transmission Electron Microscopy

Transmission electron micrographs of the kaolinites synthesized at pH_F=0.8, 3.3, 5.1, 7.4, 7.9 and 8.3 exhibit hexagonal shapes for which anisotropy increases with increasing pH_F (Figure 4), leading to-lath-shaped kaolinites for $pH_F \geq 7.4$. Fialips et al. (2000) hypothesized that the elongation of the particle is promoted by the sorption of sodium on kaolinite lateral surfaces during synthesis. The lath morphology is not common for natural kaolinite, and irregular morphologies and fine grain-size of kaolinites have usually been associated with low crystallinity (Galán et al., 1977; Brindley et al., 1986).

3.1.4. Brunauer-Emmet-Teller (BET) method and morphological parameters

The average thicknesses of the particles synthesized at different final pH values, calculated according to the Scherrer Equation and XRD data, are reported in Table 1. This parameter is equal to approximately 27 nm for samples synthesized under acidic conditions (pH_F = 0.8 and 3.3), while it decreases to ~16 nm for kaolinites prepared under the most basic conditions ($pH_F \geq 7$). These values, coupled with the average perimeter of the basal surface assessed from TEM images, allow us to calculate the specific surface areas of both lateral and basal surfaces (see Table 1). The average SSA values of the particles synthesized under acidic conditions (pH_F = 0.8 and 3.3) for lateral and basal surfaces are 6.6 m^2/g and 28.3 m^2/g, respectively. The total SSA obtained by these geometric considerations is 34.9 m^2/g, which is then higher than the BET surface area of those samples (i.e., ~24 m^2/g). Similar behavior was also found by Macht et al. (2011), who reported that the geometric surfaces calculated from the AFM images of illite particles are approximately twice the SSA measured for these particles using classical BET analysis. The authors explained this difference by the delamination of the clay particles during the sonication and dispersion of the clay in NaOH solution, which are necessary steps for AFM analysis. In this study, the kaolinite samples were gently crushed with a mortar and dispersed in distilled water using a sonication step before TEM analysis. This sample treatment may slightly increase the SSA assessed by TEM images compared with that obtained by BET analysis. For kaolinite synthesized at high pH_F (pH_F = 7.4 and 8.3), the SSA values obtained from geometric considerations are approximately 54 and 55 m^2/g for samples synthesized at pH_F = 7.4 and 8.3, respectively. The SSA for both samples obtained by the BET method is 54 m^2/g, which is in good agreement with the SSA assessed by geometric considerations. This behavior allows us to consider that our method used to assess the SSA of lateral surfaces is valid. In the literature, the total SSA of kaolinite increases with decreasing particle size (Cases et al., 1986). This latter parameter is often associated with an increase in the number of structural defects (Cases et al., 1982).

Then, the high number of defects associated with the morphology of the lath particles synthesized under basic conditions (pH_F = 7.4 and 8.3) can explained the high total SSA of these specific samples compared to the samples synthesized under more acidic conditions (pH_F = 0.8 and 3.3). The lateral specific surfaces expressed as a percentage of the total surface calculated by considering geometrical considerations are approximately 19% for samples synthesized at pH_F = 0.8 and 3.3, and they are 15% and 14% for samples prepared at pH_F = 7.4 and 8.3, respectively. These values are in the range of 12 to 54% for specific lateral surface area, expressed as a percentage of the total specific area, of most of the kaolinites reported in the literature (Cases et al., 1986).

3.1.5. Cation exchange capacity (CEC) and relation to mineralogy

The cation exchange capacity of synthetic kaolinites measured at pH = 9 is shown in Figure 5 as a function of the final synthesis pH (pH_F). The CEC of kaolinites is highly variable. Indeed, CEC values measured for samples synthesized under acid conditions ($0.8<pH_F<5.1$) are close to 1 meq/100 g whereas CEC increases dramatically to 33 meq/100 g for samples prepared under basic conditions (pH_F=8.3). Low CEC's measured for samples prepared under acid conditions tend to demonstrate that the permanent charges of these synthetic kaolinites is most likely equal to 0. This value contrasts with natural kaolinites, even those that are well-crystallized such as KGa-1b, for which the CEC due to the permanent charge is approximately 0.6 meq/100 g according to Wan and Tokunaga (2002) whereas the total CEC (due to both permanent and variable charge) of the same material can be assessed at approximately 2 meq/100 g under neutral pH conditions according to data reported by Schroth and Sposito (1997). For our samples synthesized under acid conditions

(pH_F<5.1), the CEC value measured at pH=9 is then probably due only to the contribution of edge sites (silanol and aluminol). High CEC values measured for samples synthesized under basic pH conditions may be due to the high specific surface areas of these samples or to the presence of second phases with high intrinsic CEC (Ormsby, 1962; Ma and Eggleton, 1999). Indeed, our samples synthesized under basic conditions are characterized by an SSA that is almost twice as high as the SSA of samples synthesized under acid conditions (see Table 1). Furthermore, all of our samples contain traces of pseudoboehmite (see section 3.1.1), and this mineralogical impurity may have some swelling properties in samples synthesized at pH_F>7.5 (see XRD patterns of oriented samples at low angles in Figure 6). The high CEC measured for some samples synthesized under basic conditions (from pH_F = 7.5 to pH_F = 8.3) may also be due to this swelling phase present in trace amounts in these samples. Then, Na^+/H^+ isotherms were performed only for samples for which no swelling phase, which may have a significant contribution in the total CEC of the sample, could be evidenced—that is, for samples synthesized at pH_F = 0.8, 0.9, 3.2, 3.3 and 7.4. Isotherms performed with synthetic samples obtained at pH_F = 0.8 and 0.9 were merged because of the very similar pH_F value of both samples and to ensure the availability of a sufficient amount of sample to perform isotherms. Subsequently, this material will be identified as pH_F = 0.8. Similarly, the same procedure was performed for isotherm data obtained with samples synthesized at pH_F = 3.2 and 3.3; the resulting material will be called pH_F = 3.3. The isotherm was not performed with sample synthesized at pH_F = 5.1, given the similar characteristics of this sample compared to the samples prepared under more acid conditions in terms of CEC, morphology, mineralogy and crystal chemistry.

3.2. Na^+/H^+ sorption isotherms

As mentioned in section 3.1.5, Na^+/H^+ sorption isotherms were performed for three synthetic samples characterized by the absence of a swelling phase to avoid any contribution other than kaolinite in the total CEC measured for the samples. Figure 7 shows the milliequivalent number of Na^+ sorbed as a function of pH on synthetic samples prepared at pH_F = 0.8, 3.3 and 7.4. The isotherms obtained for kaolinites synthesized at pH_F = 0.8 and 3.3 are roughly superimposed, and the sorption of Na^+ increases strongly with increasing pH, regardless of the kaolinite used. This latter statement is in agreement with previous studies considering the exchange between Na^+ and H^+ cations on clay surfaces (Nolin, 1997; Tournassat et al., 2004; Tertre et al., 2013) and is directly related to the sorption of Na^+ onto the deprotonated edges.

To assess the stability of the kaolinite surface during the determination of the Na^+/H^+ isotherm (constant edge site density), dissolution was followed through aqueous silica measurements. The mass percentages of solid dissolved during the experiments are reported as a function of pH in Figure S.I.3 (Supporting Information). The maximum value (approximately 0.5 wt%) is obtained for experiments performed under basic pH conditions (approximately pH = 10) with samples synthesized at pH_F = 7.4. With this method, we can consider that the dissolution during the Na^+/H^+ isotherm is completely negligible, whatever the pH investigated and the synthetic kaolinite used. These data, converted into percentages of edges dissolved during experiments and calculated according to the method described in section 2.2.3, are reported in Figure 8. All values are inferior to 10%, except for the data obtained at the highest pH investigated (approximately pH = 10) with the kaolinite synthesized at pH_F = 7.4. These data, combined with the consideration that the dissolution rate is likely lower than the Na^+ adsorption rate (see discussion in Tertre et al. (2006b)), lead

us to conclude that the concentration of reactive sites for sorption is constant along the Na^+/H^+ isotherms in the [4-10] pH range, a condition that is necessary to propose an ion-exchange model based on a constant sorption site density, regardless of the amount of H^+ and Na^+ sorbed onto the solid phase.

3.3 Thermodynamic modeling: effect of hexagonal/lath-shaped morphology on selectivity coefficient values.

As mentioned in section 3.2, isotherms obtained with kaolinites synthesized at pH_F = 0.8 and 3.3 (Figure 7) are roughly superimposed. Moreover, both solids have the same morphologies and specific surfaces for both basal and lateral sites (Table 1 and Figure 4). Then, we merged the two experimental data sets for these two samples, and the edge site densities as well as the selectivity coefficients between H^+ and Na^+ were assumed to be the same for these two solids. The selectivity coefficients between Na^+ and H^+ cations on pure kaolinite synthesized at pH_F = 0.8 (or 3.3) and pH_F =7.4, differing only by morphology (hexagonal-shaped *vs.* lath-shaped), are calculated using a surface complexation model without an electrostatic term. The choice to use a non-electrostatic model is supported by the fact that many of the input parameters included in surface complexation models containing electrostatic terms, as constant capacitance model or triple layer model, are not available. Such parameters are for example (a) spectroscopic information which could be used to determine the "inner" or the "outer" form of the sorbed species, (b) electrokinetic data to assess surface potentials, and which could be different for the different crystallographical faces presented for our particles and (c) the lack of knowledge concerning the site density and associated acidity constants (pKa) of the different functional groups located on the different faces of our particles. This choice has been performed also by several others authors, as

Bradbury and Baeyens (1997) and Tournassat et al. (2004), who demonstrated that non-electrostatic models could be used with success to interpret experimental sorption data. For the calculations, the Phreeqc® software (Parkhurst et al., 1999) is used in association with the minteqv4 thermodynamic data base. We assume that Na^+ and H^+ cations are sorbed only on the lateral edge sites of the kaolinites and that our samples have no permanent charge. This latter assumption is supported by the very low amounts of Na^+ sorbed at pH around 6, and which are equal to around 0.06 and 0.18 meq/100 g for hexagonal and lath particles, respectively. Indeed, these values correspond to 6 and 2 % of the total CEC's measured at pH=9 for hexagonal and lath particles respectively, and then lead us to assume with a good confidence that there is no permanent charge in our samples. Such assumption is also supported by the absence of swelling layers, which could reflect the presence of a significant permanent charge, evidenced by the XRD analysis (see section 3.1.5). For edge sites of hexagonal particles, we suppose that there is the same contribution of the three faces: (010), (110) and (1-10), whereas only the contribution of the exacerbated face was assumed for lath particles: (010) face. According to the edge site densities proposed by Koretsky et al. (1998) for each of these faces (in sites/nm^2) and the specific surface of the lateral sites estimated in this study for particles with both morphologies (in m^2/g) (see Table 1), the total edge site densities are calculated to be equal to 11.7 and 20 meq/100 g for hexagonal and lath-shaped particles, respectively. In our approach, we do not consider the reactivity of the aluminol sites located in the gibbsite sheet due to the coordination of the Al atoms, leading to no reactivity at such sites in the [4, 10] pH range (see discussions in Huertas et al. (1998) and Tertre et al. (2006a)). Moreover, for simplicity, the silanol and aluminol edge sites are merged into a single site, and we assume that oxygen atoms belonging to these edge sites are linked to only one metal atom (e.g., >AlOH), although a higher coordination number is sometimes mentioned in the literature as $>Al_2OH_2^{0.5+}$ (Bolt and van Riemsdijk, 1982). This single site is

identified as the >SOH site in Table 2 and is characterized by protonation/deprotonation constants that are fixed, regardless of the shape of the particle. This latter assumption is supported by the absence of studies reporting such constants for the different crystallographic faces (e.g., (010), (110)) of a kaolinite exposed to an aqueous environment). The proportion of silanol and aluminol sites on the different crystallographic faces is not available in the literature, to our knowledge; this limitation also supports the fact to merge the different edge sites in a single site. Values chosen for the protonation and deprotonation constants of the >SOH site are taken from the literature for the aluminol/silanol sites of kaolinite edges. Our approach assumes that the protonation of silanol sites does not occur in the pH range investigated, as demonstrated in Tertre et al. (2006a); thus, the protonation constant for the >SOH site is assumed to be that of the aluminol sites. For this latter parameter, the value proposed by Brady et al. (1996) is chosen (i.e., log Kc=2.3; see Table 2). Furthermore, the value chosen for the deprotonation constant of the >SOH site corresponds to an average value reported in the literature for both silanol and aluminol sites (Brady et al., 1996 and Tertre et al., 2006a) (i.e., log Kc = -7.0; see Table 2). Indeed, Brady et al. (1996) proposed values close to -5.3 and -8.2 for aluminol and silanol edge sites, respectively, while Tertre et al. (2006a) reported log Kc = -6.1 and -7.7 for these two sites. Note that we are aware (1) that other protonation/deprotonation constants than those used in this study are available in literature to describe the reactivity of the functional groups located onto the edges of kaolinite particles, and (2) that pKa chosen in this study are probably not fully representative of the acidity properties of our material. However, our problematic is not to obtain such parameters, but to probe the influence of the particle morphology on the exchange between two cations (Na^+ and H^+ in our case) towards kaolinite surfaces. Then, using the same pKa values for both morphologies allow us to bring some information relative to this question. With these assumptions, a value of log Kc(Na^+/H^+) equal to -5.5 is required to interpret experimental

data obtained using hexagonal-shaped particles, whereas for lath-shaped particles (or more anisotropic hexagonal particles), log $Kc(Na^+/H^+)$ equal to -4.7 is needed. A comparison between the experimental and predicted data is reported in Figure 9A, while the model is described in Table 2. To test the sensibility of the model, the value describing the experimental data obtained with the hexagonal particles (log $Kc(Na^+/H^+)$ of -5.5) is used to predict a Na^+/H^+ sorption isotherm with lath-shaped particles (see Figure 9B). The results show that the selectivity coefficient proposed to interpret the experimental data obtained with hexagonal particles cannot accurately describe the data obtained with lath-shaped particles. This behavior supports the fact that ion-exchange reactions between Na^+ and H^+ depend strongly on the morphology of the particles. However, this dependence is not necessary due to the sole possible variation of the Na^+/H^+ selectivity coefficient with the particle morphology, as demonstrated above. Indeed, different assumptions were performed in our modeling approach, as the fact to take the same values for the protonation/deprotonation constants of the edge sites for both morphologies of particles (hexagonal and lath-shaped). Some authors have indicated that the reactivity of the different crystallographic faces of clay minerals in an aqueous environment could differ, for example, in dissolution experiments (see the studies of Bickmore et al. (2001) for hectorite and nontronite, and references therein). Moreover, some authors have calculated by combining bond valence theory and quantum mechanical calculations, such protonation/deprotonation constants (Bickmore et al., 2003; Churakov, 2006; Liu et al., 2013). However, none of these studies has calculated these constants for the different crystallographic faces of kaolinite. If the variation of these constants with crystallographic face was identified, it could also explain the possible variation of the Na^+/H^+ selectivity coefficient with the particle morphology evidenced in this present study. Note however that globally, ion-exchange reactions between Na^+ and H^+ cannot be described with the same model for hexagonal and lath particles, and the

morphology of the kaolinite particles should be taken into account to describe the data obtained from Na^+/H^+ ion-exchange experiments accurately.

4. Conclusions and perspectives

This study is devoted to highlighting the effect of the morphology of clayey particles on their sorption properties towards two inorganic cations (H^+ and Na^+). Kaolinites synthesized hydrothermally at $pH_F<7.5$ are characterized by different morphologies (hexagonal vs. lath-shaped particles) and the absence of a swelling phase. This latter information, associated with the fact that there is no sorption of Na^+ on any synthetic kaolinites until a pH of approximately 7, suggests that there is no permanent charge in the samples. Then, a dramatic increase of the sorption of Na^+ is observed for pH>7, regardless of the morphology of the kaolinite particles; this increase is attributed to sorption onto the edge sites. With edge site densities calculated from both the specific surface of lateral sites and crystallographic data for the (010), (110) and (1-10) faces, a selectivity coefficient for interpretation of the experimental Na^+/H^+ isotherms, obtained with a surface complexation model, is proposed. The results show that the selectivity coefficient between Na^+ and H^+ cations could be strongly dependent on the morphology of the kaolinite particles. Then, the morphology of the particles is a key parameter to consider in all geochemical models incorporating sorption reactions on clay particles.

Although this study clearly demonstrates that the selectivity coefficient between two cations depends on the particle morphology (hexagonal vs. lath-shaped), the question remains whether the evolution of the affinity between the two cations is continuous when hexagonal particles become increasingly anisotropic. Other Na^+/H^+ isotherms could be obtained with

kaolinites synthesized at pH_F values between 5.1 and 7.4, corresponding to a pH_F range for which morphology changes drastically. Furthermore, experimental data could be interpreted with a more detailed mechanistic approach by introducing additional constraints into the surface complexation model, such as the exact contribution of each of the different edge sites located on each face of the particle and the protonation/deprotonation constant for each of these sites. These parameters could be partially obtained using the periodic bond chain theory to predict the topology of the functional groups located on the different edge faces of a particle. Molecular modeling methods could also be used to obtain the acidity of each of the edge groups located on the main different crystallographic faces evidenced in this study, as performed by Bickmore et al. (2003) and Churakov (2006) for pyrophyllite.

Acknowledgments

The authors gratefully acknowledge Emile Bere and Jean-Dominique Comparot (IC2MP, Poitiers) for their help in TEM and BET analyses, respectively. The manuscript was much improved by the constructive comments of two anonymous reviewers.

Supplementary information

Supplementary data associated with this article can be found in the online version at XXX.

References

Bhattacharyya, K.G., and Gupta, S.S., 2008. Sorption of a few heavy metals on natural and modified kaolinite and montmorillonite: A review. Advances in Colloid and Interface Science 140, 114–131.

Bi, Y., Li, D., and Nie, H., 2010. Preparation and catalytic properties of tungsten oxides with different morphologies. Materials Chemistry and Physics 123, 225-230.

Bickmore, B.R., Bosbach, D., Hochella, M.F., Jr., Charlet, L., and Rufe, E., 2001. In situ atomic force microscopy study of hectorite and nontronite dissolution: Implications for phyllosilicate edge surface structures and dissolution mechanisms. American Mineralogist 86, 411-423.

Bickmore, B.R., Rosso, K.M., Nagy, K.L., Cygan, R.T., and Tadanier, C.J., 2003. Ab initio determination of edge surface structures for dioctahedral 2:1 phyllosilicates: implications for acid-base reactivity. Clays and Clay Minerals 51, 359-371.

Bolt, G., and van Riemsdijk, W.H., 1982. In: G. Bolt (ed.), Soil Chemistry. B. 254 Physico-chemical models. Second ed., Elsevier.

Bradbury, M.H. and Baeyens, B., 1997. A mechanistic description of Ni and Zn sorption on Na–montmorillonite. Part II: modeling. Journal of Contaminant Hydrology 27, 223–248.

Brady, P.V., Cygan, R.T. and Nagy, K.L., 1996. Molecular controls on kaolinite surface charge. Journal of Colloid and Interface Science 183, 356-364.

Brigatti, M.F., Galan, E., and Theng, B.K.G., 2006. Structure and mineralogy of clay minerals. In: Bergaya, F., Theng, G.K.B., Lagaly, G. (Eds.), Handbook of clay science. Developments in Clay Science, vol. 1. Elsevier, Amsterdam, pp. 19–86.

Brindley, G.W., and Brown, G., 1980. Crystal structures of clay minerals and their X-ray identification. Mineralogical Society, London.

Brindley, G.W., Chih-chun, K., Harrison, J.L., Lipsicas, M. and Raythatha, R., 1986. Relations between structural disorder and other characteristics of kaolinites and dickites. Clays and Clay Minerals 34, 239-249.

Brunauer, S., Emmett, P.H. and Teller, E.J., 1938. Sorption of gases in multimolecular layers. Journal of American Chemical Society 60, 309-318.

Buttle, J.M., and C.F., Labadia., 1999. Deicing salt accumulation and loss in highway snowbanks. Journal of Environmental Quality 28, 155-164.

Cases, J.M., Liétard, O., Yvon, J., and Delon, J.F., 1982. Etude des propriétés cristallographiques, morphologiques et superficielles de kaolinites désordonnées. Bulletin de Minéralogie 105, 439-457.

Cases, J. M., Cunin, P., Grillet, Y., Poinsigon, C. and Yvon, J., 1986. Methods of analyzing morphology of kaolinites: relations between crystallographic and morphological properties. Clay Minerals 21, 55-68.

Cleary, R.W., 1978. Pollution of groundwater. In water problems of urbanizing areas, proceedings of the research conference, New England College, Henniker, New Hampshire, July 16-21, 1978. The American Society of Civil Engineers, New York. pp. 134-142.

Churakov, S.V., 2006. Ab initio study of sorption on pyrophyllite: structure and acidity of the edge sites. Journal of Physical Chemistry B 110, 4135-4146.

Dudkin, B.N., Loukhina, I.V., Isupov, V.P. and Avvakumov, E.G., 2005. Mechanical activation of kaolinite in the presence of concentrated sulfuric acid. Russian Journal of Applied Chemistry 78, 33-37.

Farmer, V.C., 1974. The Infrared Spectra of Minerals. Mineralogical Society, London.

Fialips, C.I., Petit, S., Decarreau, A., and Beaufort, D., 2000. Influence of synthesis pH on the kaolinite crystallinity and surface properties. Clays and Clays Minerals 48, 173-184.

Galán, E., Mattias, P.P. and Galván, J., 1977. Correlation about kaolin genesis and age of some Spanish kaolinites. Processing of 8th International Kaolin Symposium and Meeting on Alunite. Madrid-Rome, K-8, 8 pp.

Gu, X., and Evans, L.J., 2008. Surface complexation modeling of Cd(II), Cu(II), Ni(II), Pb(II) and Zn(II) sorption onto kaolinite. Geochimica et Cosmochimica Acta 72, 267-276.

Hassan, M.S., Villiéras, F., Razafitianamaharavo, A., and Michot, L.J., 2005. Role of exchangeable cations on geometrical and energetic heterogeneity of kaolinites. Langmuir 21, 12283-12289.

Hinckley, D.N., 1963. Variability in crystallinity values among the kaolin deposits of the coastal plain of Georgia and South Carolina. Clays and Clay minerals 11, 229-235.

Huertas, J.F., Chou, L. and Wollast, R., 1998. Mechanism of kaolinite dissolution temperature and pressure: Part 1. Surface speciation. Geochimica et Cosmochimica Acta 62, 417–431.

Iriarte, B., Petit, S., Huertas, F.J., Fiore, S., Grauby, O., Decarreau, A., and Linares, J., 2005. Synthesis of kaolinite with a high level of Fe^{3+} for Al substitution. Clays and Clay Minerals 53, 1-10.

Johnston, C.T., and Tombácz, E., 2002. Surface chemistry of soil minerals. In: soil mineralogy with environmental applications (Eds. Dixon, J.B., Schulze, D.G.). Soil Science Society of America, Madison, Wisconsin, USA, pp. 37–67.

Koretsky, C.M., Sverjensky, D.A., and Sahai, N., 1998. A model of surface site types on oxide and silicate minerals based on crystal chemistry: Implications for site types and

densities, multi-site sorption, surface infrared spectroscopy, and dissolution kinetics. American Journal of Science 298, 349-438.

Langford, J.I., and Wilson, A.J.C., 1978. Scherrer after sixty years. A survey and some new results in the determination of crystallite size. Journal of Applied Crystallography 11, 102-113.

Liétard, O., 1977. Contribution á l'étude des propriétés physicochimiques, cristallographiques et morphologiques des kaolins. Ph. D. Thesis, University of Nancy.

Liu, X., Lu, X., Sprik, M., Cheng, J., Meijer, E.J., and Wang, R., 2013. Acidity of edge surface sites of montmorillonite and kaolinite. Geochimica et Cosmochimica Acta 117, 180-190.

Ma, C., and Eggleton, R.A., 1999. Cation exchange capacity of kaolinite. Clays and Clay Minerals 47, 174–180.

Macht, F., Eusterhues, K., Pronk, G.J., and Totsche, K.U., 2011. Specific surface area of clay minerals: Comparison between atomic force microscopy measurements and bulk-gas (N_2) and -liquid (EGME) sorption methods. Applied Clay Science 53, 20–26.

Madejova, J., Balan, E., and Petit, S., 2011. Application of vibrational spectroscopy to the characterization of phyllosilicates and other industrial minerals. In Advances in the characterization of industrial minerals (ed. Christidis). European Mineralogical Union Notes in Mineralogy 9, chapter 6, 171-226.

Miranda-Trevino, J.C., and Coles, C.A., 2003. Kaolinite properties, structure and influence of metal retention on pH. Applied Clay Science 23, 133–139.

Miyawaki, R., Tomura, S., Samejima, S., Okazaki, M., Izuta, H., Muruyama, S.I., and Shibasaki, Y., 1991. Effects of solution chemistry on the hydrothermal synthesis of kaolinite. Clays and Clay minerals 39, 498-508.

Nolin, D., 1997. Rétention de radioéléments à vie longue par des matériaux argileux. Influence d'anions contenus dans les eaux naturelles. Ph. D. Thesis, University of Paris 6.

Ormsby, W.C., Shartsis, J.M., and Woodside, K.H., 1962. Exchange behavior of kaolins of varying degrees of crystallinity. Journal of the American Ceramic Society 45, 361-366.

Parkhurst, D.L., and Appelo, C.A.J., 1999. Phreeqc2 user's manual and program, US Geological Survey. Available at: <http://www.geo.vu.nl/users/posv/phreeqc.html>.

Petit, S., and Decarreau, S., 1990. Hydrothermal (200 °C) synthesis and crystal-chemistry of iron-rich kaolinites. Clay Minerals 25, 181-196.

Satokawa, S., Osaki, Y., Samejima, S., Miyawake, R., Tomura, S., Sjobasalo, U. and Sigahara. Y., 1994. Effects of the structure of silica-alumina gel on the hydrothermal synthesis of kaolinite. Clays and Clay Minerals 42, 288-297.

Schroth, B.K., and Sposito, G., 1997. Surface charge properties of kaolinite. Clays and Clay Minerals 45, 85–91.

Strickland, J.D.H., Parsons, T.R., 1972. Determination of reactive silicate. A Practical Handbook of Seawater Analysis. Fisheries Research Board of Canada Bulletin, Ottawa, pp. 65-70.

Tertre, E., Castet, S., Berger, G., Loubet, M. and Giffaut, E., 2006a. Surface chemistry of kaolinite and Na-montmorillonite in aqueous electrolyte solutions at 25 and 60°C: Experimental and modeling study. Geochimica et Cosmochimica Acta 70, 4579-4599.

Tertre, E., Berger, G., Simoni, E., Castet, S., Giffaut, E., Loubet, M., and Catalette, H., 2006b. Europium retention onto clay minerals from 25 to 150°C: experimental measurements, spectroscopic features and sorption modelling. Geochimica et Cosmochimica Acta 70, 4563-4578.

Tertre, E., Prêt, D., and Ferrage, E., 2011. Influence of the ionic strength and solid/solution ratio on Ca(II)-for-Na^+ exchange in montmorillonite. Part 1: Chemical measurements, thermodynamic modeling and implications for trace elements geochemistry. Journal of Colloid and Interface Science 353, 248-256.

Tertre, E., Hubert, F., Bruzac, S., Pacreau, M., Ferrage, E. and Pret, D., 2013. Ion-exchange reactions on clay minerals coupled with advection/dispersion processes. Application to Na^+/Ca^{2+} exchange on vermiculite: Reactive-transport modeling, batch and mix-flow reactor experiments. Geochimica et Cosmochimica Acta 112, 1-19.

Tournassat, C., Ferrage, E., Poinsignon, C. and Charlet, L., 2004. The titration of clay minerals II. Structure-based model and implications for clay minerals. Journal of Colloid and Interface Science 273, 234-246.

Tsuzuki, Y., 1976. Solubility diagrams for explaining zone sequences in bauxite, kaolin and pyrophyllite-diaspore deposits. Clays and Clay Minerals 24, 297-302.

Wan, J., and Tokunaga, T.K., 2002. Partitioning of clay colloids at air-water interfaces. Journal of Colloid and Interface Science 247, 54-61.

Wypych, F. and Satyanarayana, K.G., 2004. Clay Surfaces. Interface Science and Technology-Volume 1, Elsevier Academic Press. UK.

Zhang, L., Xu, T., Zhao, X., and Zhu, Y., 2010. Controllable synthesis of Bi_2MoO_6 and effect of morphology and variation in local structure on photocatalytic activities. Applied Catalysis B: Environmental 98, 138-146.

Table Captions

Table 1. Specific surfaces obtained from geometrical considerations for both lateral and basal surfaces and BET surface area measured for some synthetic kaolinites.

Table 2. Selectivity coefficients proposed in this study with a surface complexation model to interpret experimental Na^+/H^+ isotherms obtained with hexagonal and lath particles of pure kaolinites. Associated edge site densities assessed from the surface area of lateral sites and crystallography data are 11.7 and 20 meq/100 g for hexagonal and lath shaped particles, respectively (see text for detailed explanations).

Figure Captions

Figure 1. XRD patterns (bulk powder) of Starting Material (SM) and synthesized kaolinites (pH_F: pH measured at the end of synthesis; PB= pseudo-boehmite).

Figure 2. Size of the coherent domain of the synthetic kaolinites plotted as a function of the final pH of synthesis (pH_F). Data are calculated with d_{001} (A) and d_{060} reflections (B) obtained from XRD patterns recorded for bulk samples.

Figure 3: FTIR spectra of Starting Material (SM) and synthetic kaolinites as a function of the final pH of synthesis (pH_F).

Figure 4. Transmission electron micrographs of synthetic kaolinites differing by their final pH of synthesis (pH_F).

Figure 5. Cation-exchange capacities of synthetic kaolinites measured at pH = 9 as a function of the final pH of synthesis (pH_F).

Figure 6. XRD patterns (oriented preparations) of kaolinites synthesized at pH_F 7.4, 7.5 and 8.3; AD = recording in air-dried conditions and EG = recording in an atmosphere saturated with ethylene glycol; pH_F: pH measured at the end of synthesis; PB= pseudo-boehmite.

Figure 7. Na^+/H^+ sorption isotherms measured for synthetic kaolinites synthesized at pH_F 0.8, 3.3 and 7.4.

Figure 8. Percentage of edges dissolved as a function of the equilibrium pH measured all along the Na^+/H^+ isotherms performed with three synthetic kaolinites differing by their final pH of synthesis (pH_F). These data are obtained from measurements of aqueous silica concentrations.

Figure 9. (A) Comparison between experimental data and fitted data using a surface complexation model without an electrostatic term for Na^+/H^+ sorption isotherms obtained with hexagonal and lath-shaped particles. (B) Sensibility effect of the log $Kc(Na^+/H^+)$ value used in the model to predict Na^+/H^+ isotherm with lath-shaped particles. For predicted curves, edge site densities are fixed and calculated from the morphology of the particles (specific surfaces of lateral sites) and crystallography data for (010), (110) and (1-10) faces based on the data of Korestsky et al. (1998).

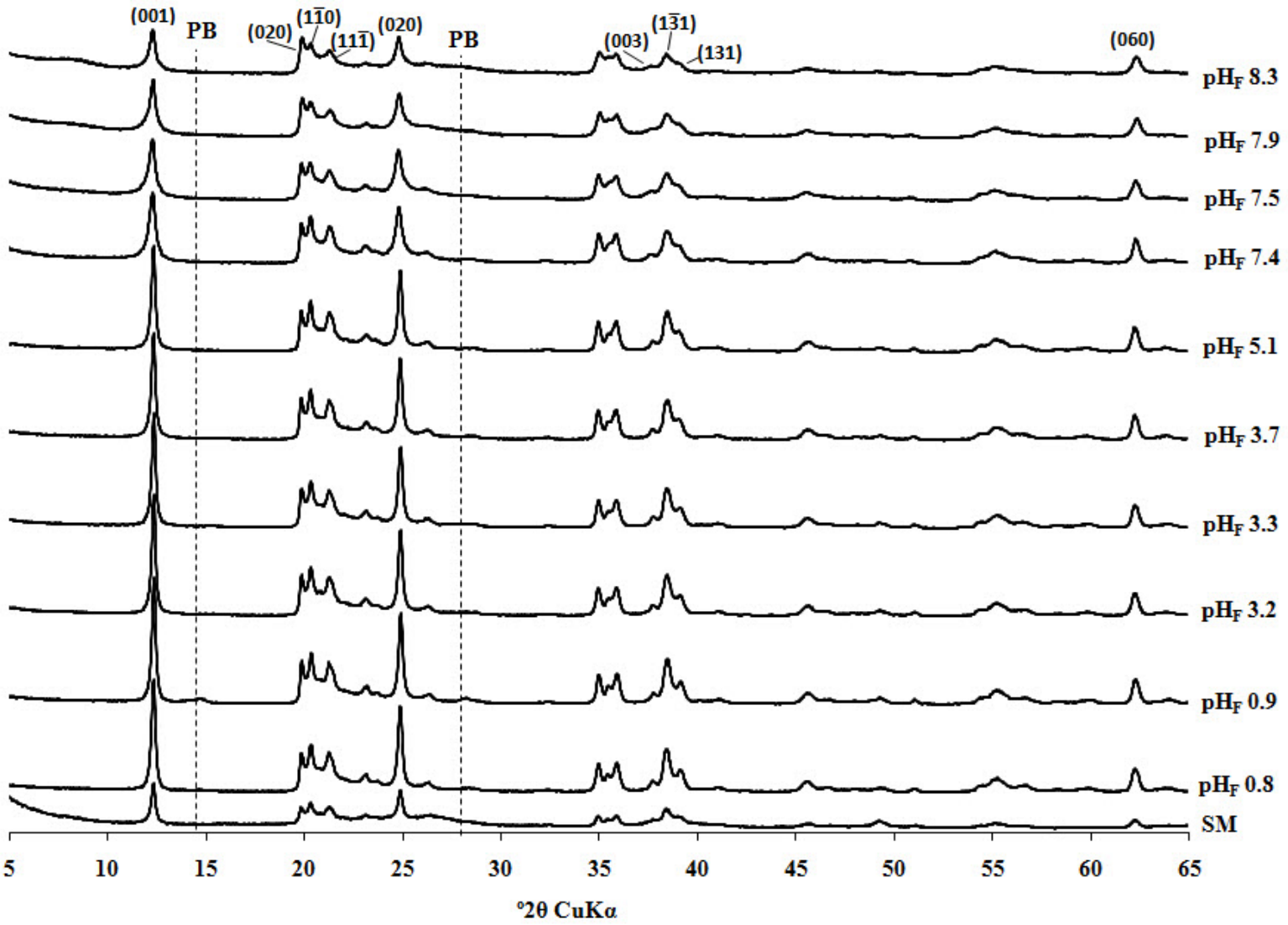
(001)
PB
(020)
(1$\bar{1}$0)
(11$\bar{1}$)
(020)
PB
(003)
(1$\bar{3}$1)
(131)
(060)
pH$_F$ 8.3
pH$_F$ 7.9
pH$_F$ 7.5
pH$_F$ 7.4
pH$_F$ 5.1
pH$_F$ 3.7
pH$_F$ 3.3
pH$_F$ 3.2
pH$_F$ 0.9
pH$_F$ 0.8
SM
5
10
15
20
25
30
35
40
45
50
55
60
65
°2θ CuKα

Figure 1

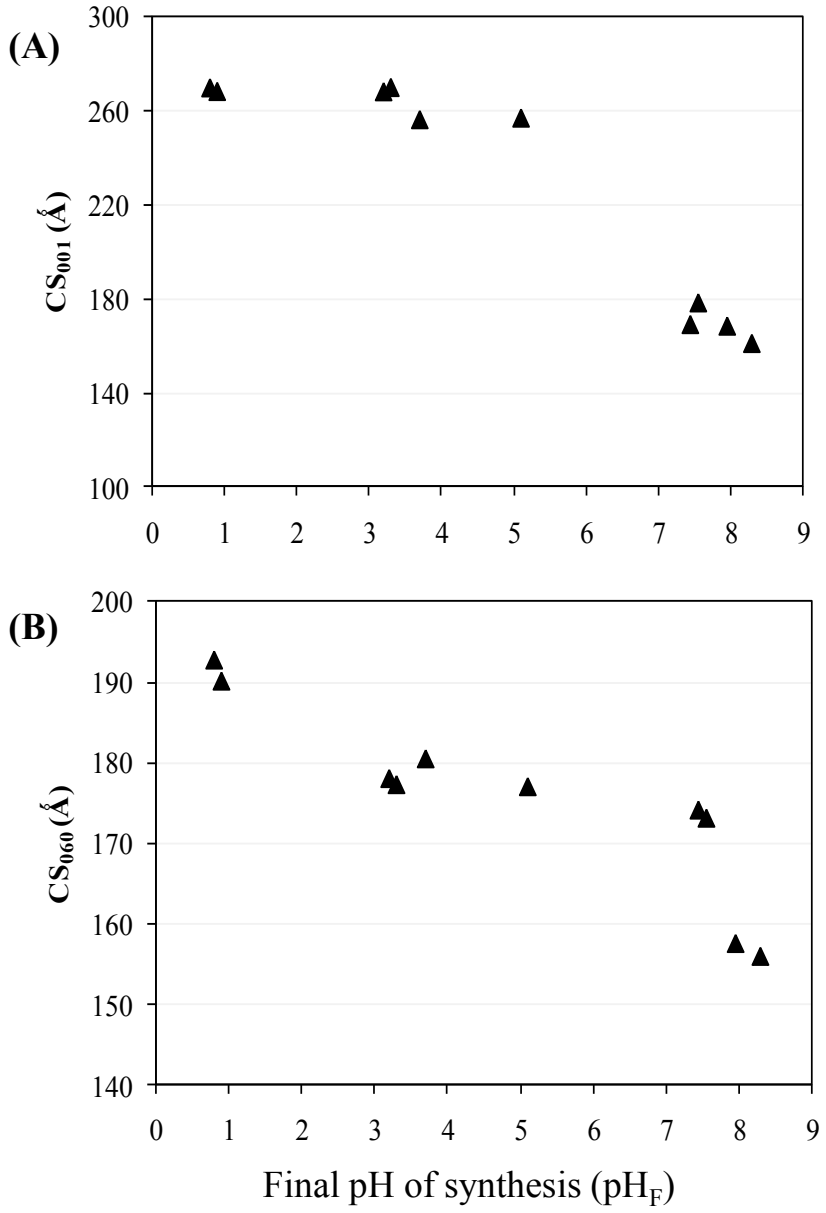
(A)
300
260
220
180
140
100
CS_{001} (Å)
0
1
2
3
4
5
6
7
8
9
(B)
200
190
180
170
160
150
140
CS_{060} (Å)
0
1
2
3
4
5
6
7
8
9
Final pH of synthesis (pH_F)

Figure 2

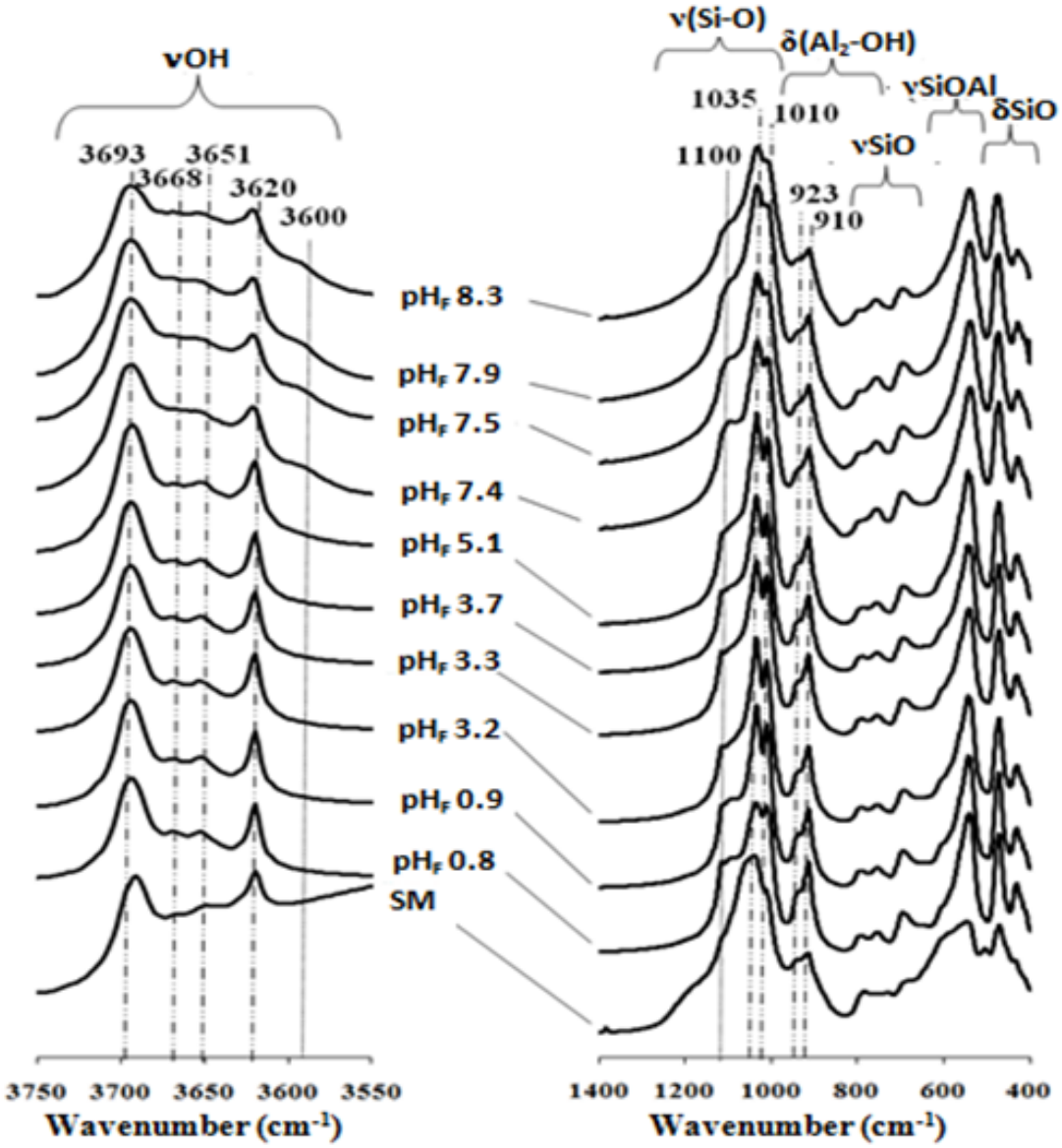
νOH
3693
3651
3668
3620
3600
pH_F 8.3
pH_F 7.9
pH_F 7.5
pH_F 7.4
pH_F 5.1
pH_F 3.7
pH_F 3.3
pH_F 3.2
pH_F 0.9
pH_F 0.8
SM
3750 3700 3650 3600 3550
Wavenumber (cm-1)
ν(Si-O)
δ(Al2-OH)
νSiOAl
δSiO
1035
1010
1100
νSiO
923
910
1400 1200 1000 800 600 400
Wavenumber (cm-1)

Figure 3

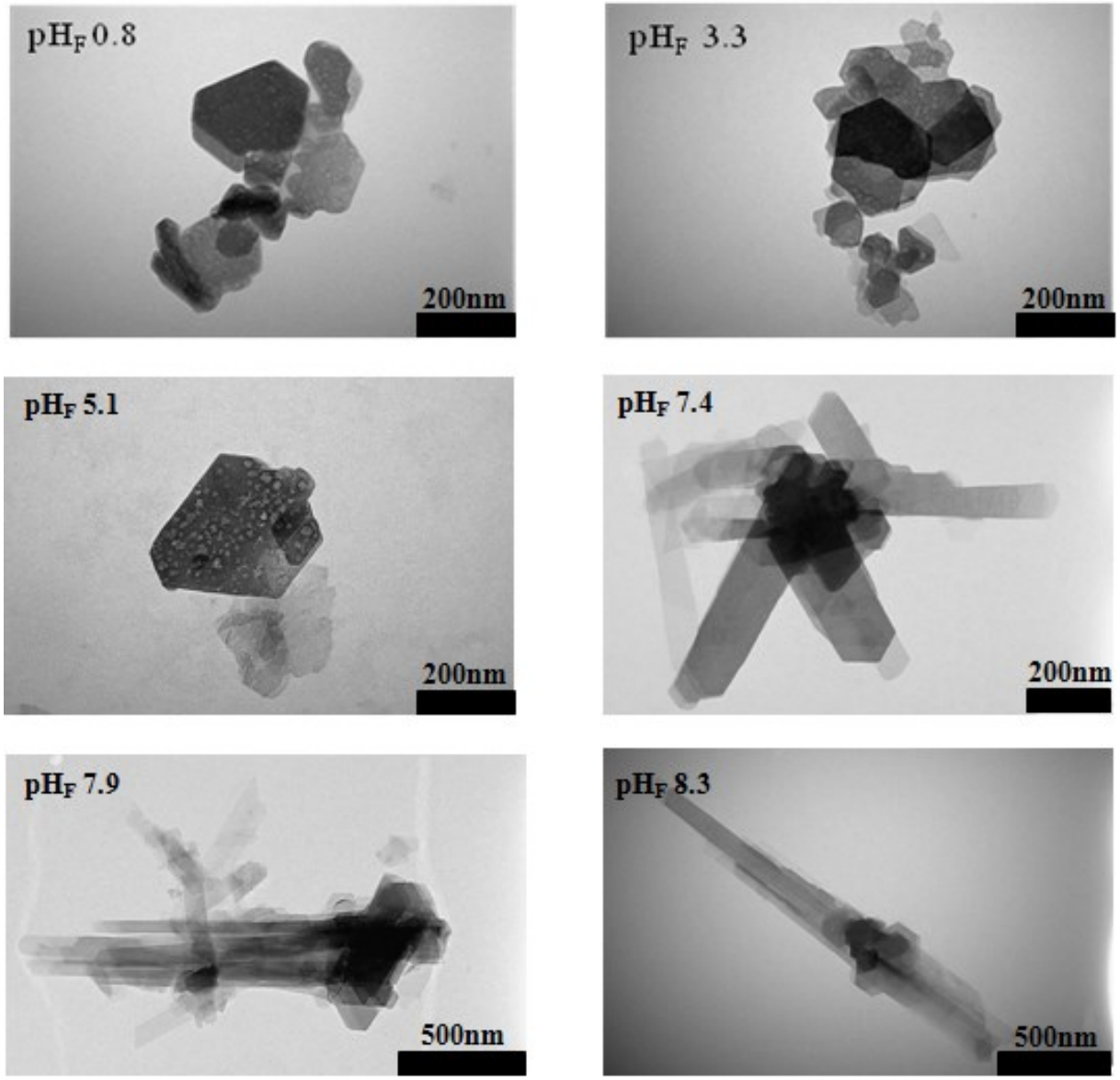
pH$_F$ 0.8
200nm
pH$_F$ 3.3
200nm
pH$_F$ 5.1
200nm
pH$_F$ 7.4
200nm
pH$_F$ 7.9
500nm
pH$_F$ 8.3
500nm

Figure 4

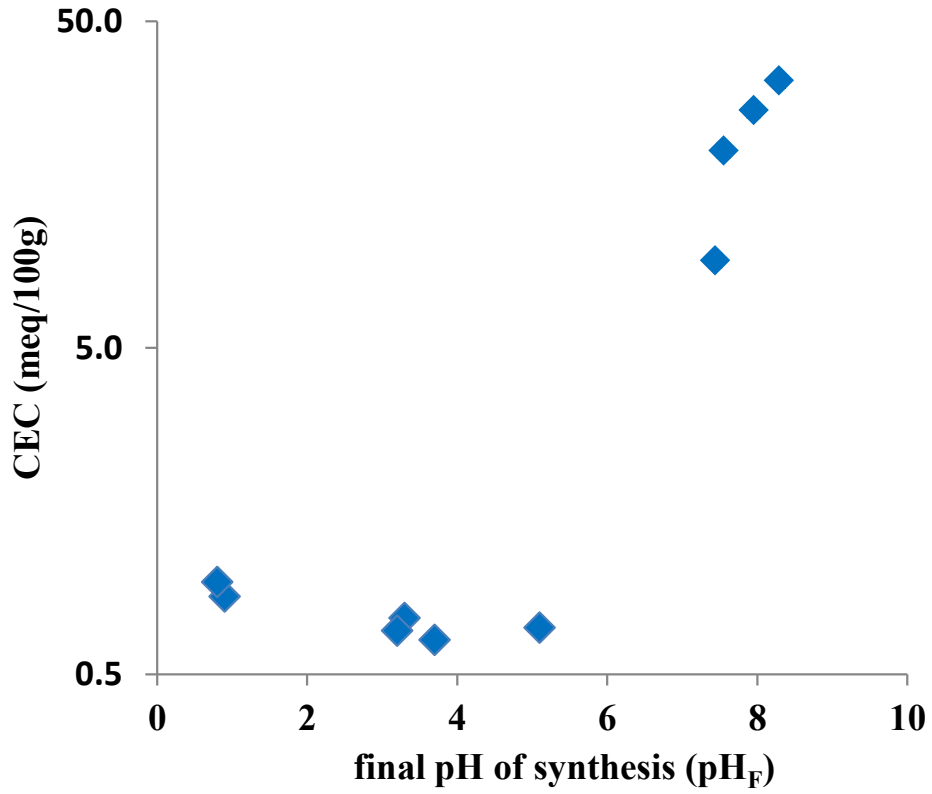

Figure 5

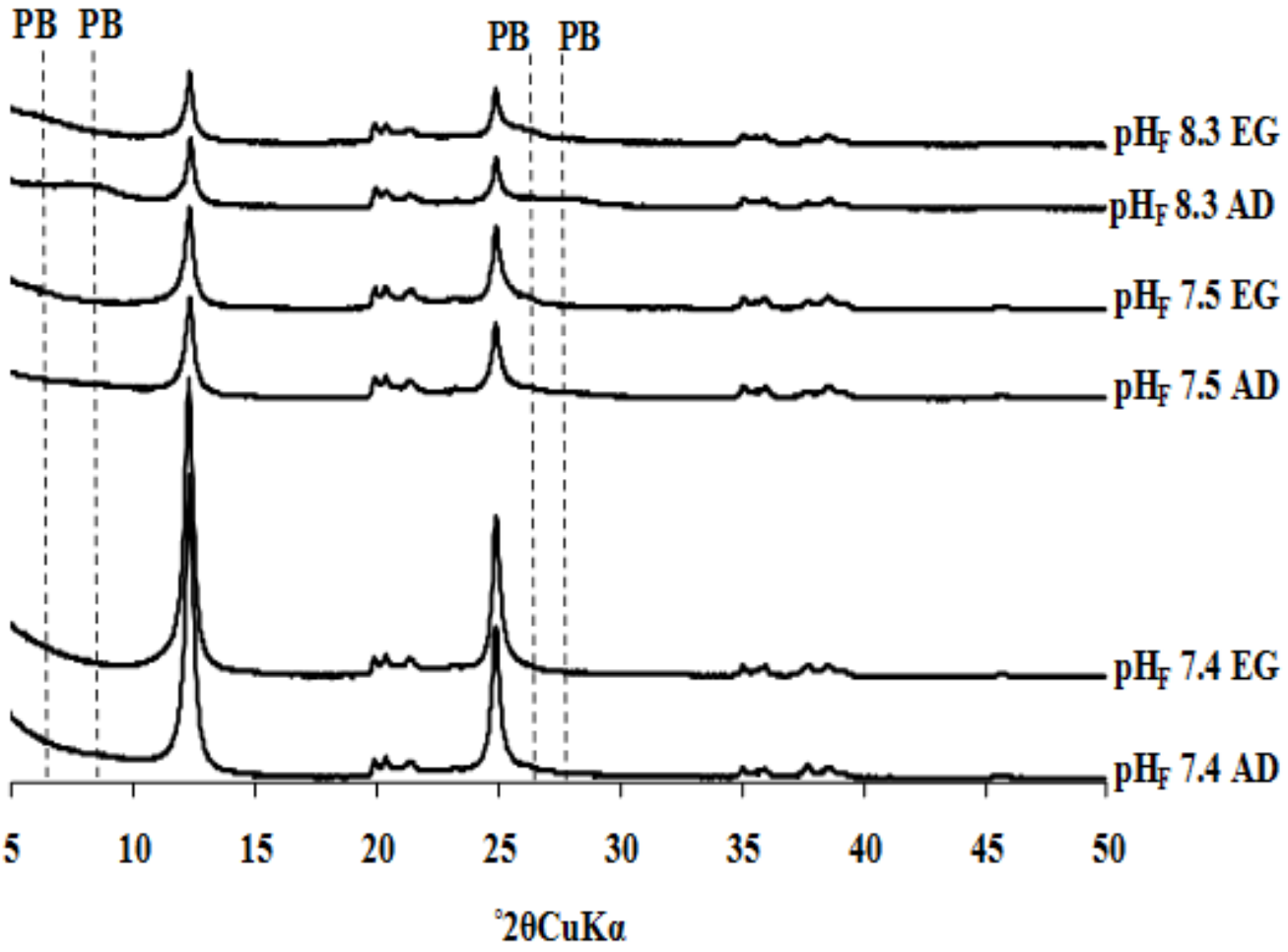
PB
PB
PB
PB
pH$_F$ 8.3 EG
pH$_F$ 8.3 AD
pH$_F$ 7.5 EG
pH$_F$ 7.5 AD
pH$_F$ 7.4 EG
pH$_F$ 7.4 AD
5
10
15
20
25
30
35
40
45
50
°2θCuKα

Figure 6

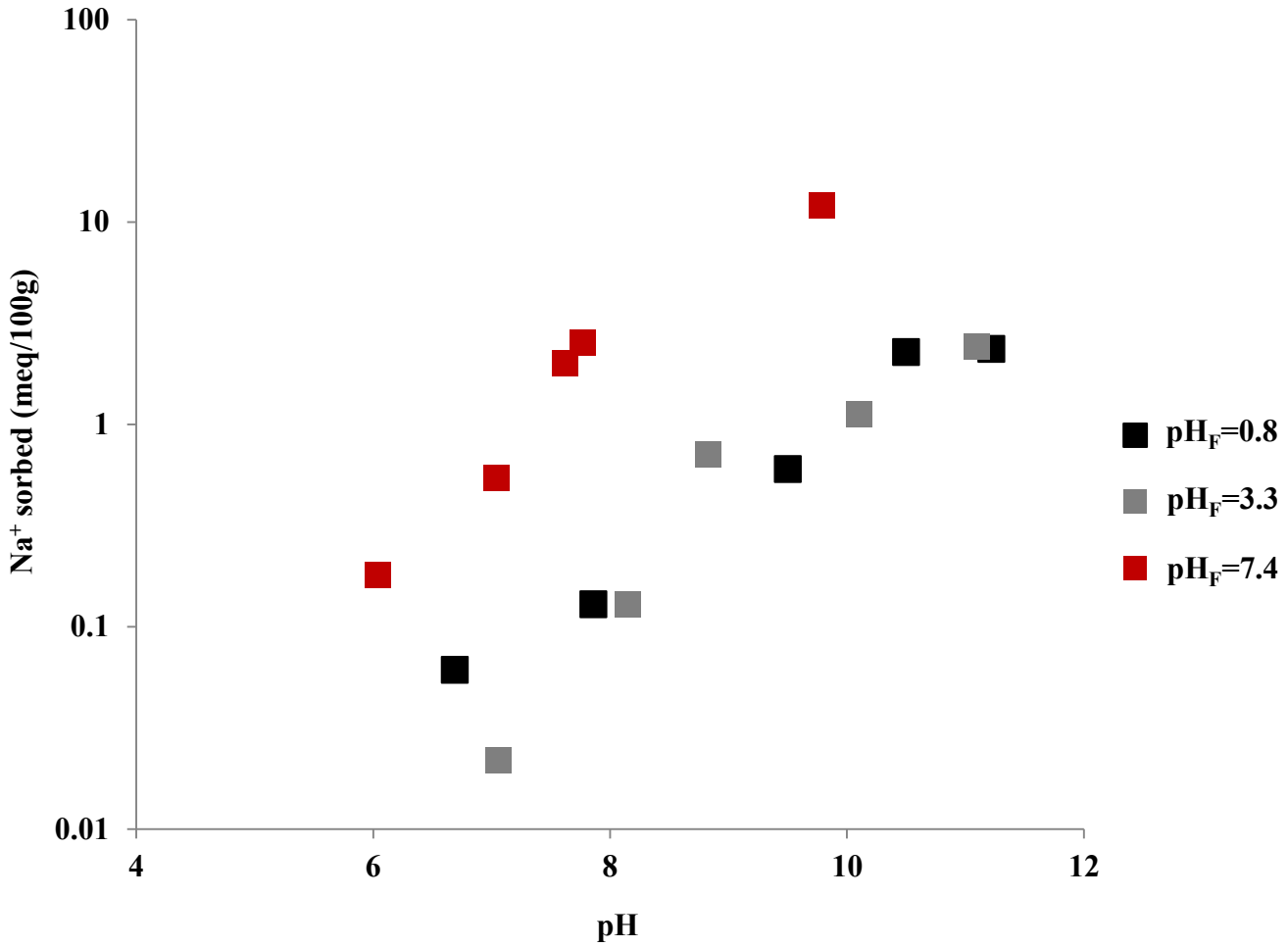
100
10
1
0.1
0.01
Na+ sorbed (meq/100g)
4
6
8
10
12
pH
pHF=0.8
pHF=3.3
pHF=7.4

Figure 7

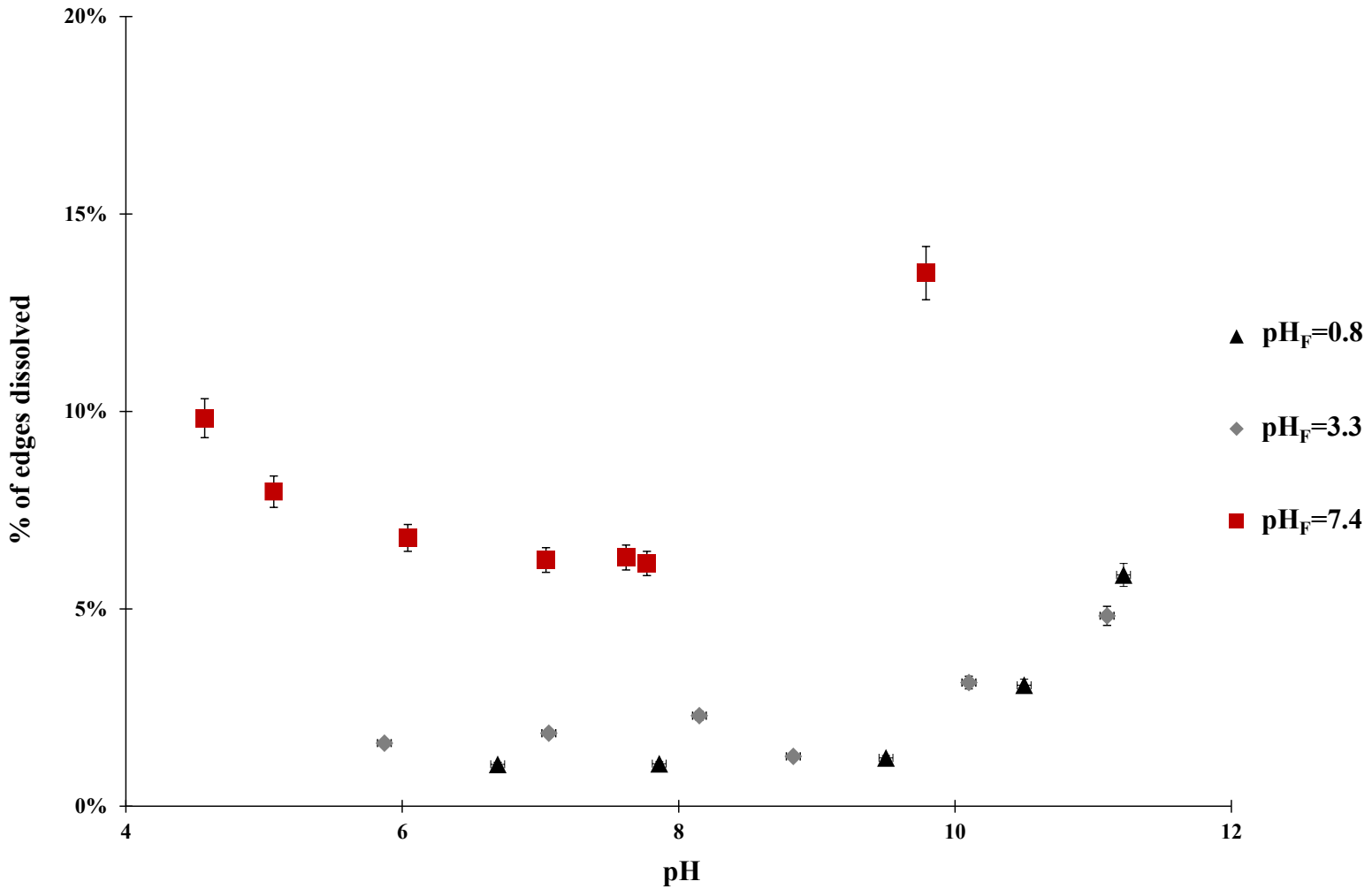

Figure 8

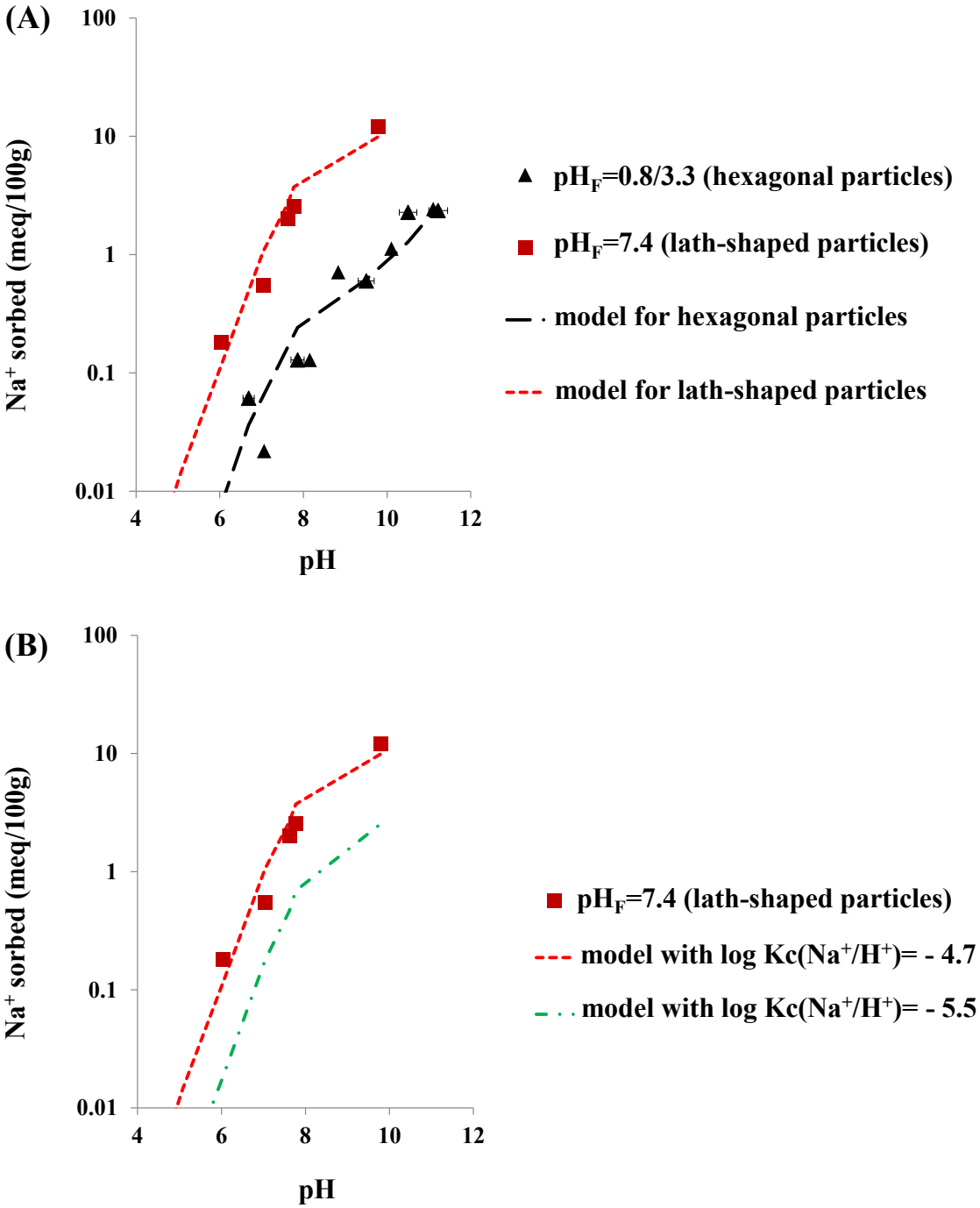
(A)
100
10
1
0.1
0.01
Na+ sorbed (meq/100g)
4
6
8
10
12
pH
pHF=0.8/3.3 (hexagonal particles)
pHF=7.4 (lath-shaped particles)
model for hexagonal particles
model for lath-shaped particles
(B)
100
10
1
0.1
0.01
Na+ sorbed (meq/100g)
4
6
8
10
12
pH
pHF=7.4 (lath-shaped particles)
model with log Kc(Na+/H+)= - 4.7
model with log Kc(Na+/H+)= - 5.5

Figure 9

Table 1. Specific surfaces obtained from geometrical considerations for both lateral and basal surfaces and BET surface area measured for some synthetic kaolinites.

Samples	average basal surface (nm^2)	Full-Width Half-Maximum at d_{001} peak [FWHM (°2θ)]	average thickness (nm)	average lateral surface (nm^2)	average specific surface for lateral surfaces (m^2/g)	average specific surface for basal surfaces (m^2/g)	total surface obtained considering geometric considerations (m^2/g)	BET surface (m^2/g)
pH_F 0.8	34640	0.296	27	16200	6.6	28.3	34.9	23.1
pH_F 3.3	51961	0.296	27	24300	6.6	28.3	34.9	24.1
pH_F 7.4	65550	0.475	16.7	23046	8	45.7	53.7	54
pH_F 8.3	91500	0.499	16.1	29463	7.6	47.4	55	54

Table 2. Selectivity coefficients proposed in this study with a surface complexation model to interpret experimental Na^+/H^+ isotherms obtained with hexagonal and lath particles of pure kaolinites. Associated edge site densities assessed from the surface area of lateral sites and crystallography data are 11.7 and 20 meq/100 g for hexagonal and lath shaped particles, respectively (see text for detailed explanations).

Ion-exchange reaction	log Kc (25°C)	Observations
$H^+ + >SOH = >SOH_2^+$	2.3	The value is given for aluminol site by Brady et al. (1996).
$>SOH = >SO^- + H^+$	-7.0	An average value between the deprotonation value for both aluminol and silanol sites (Brady et al., 1996 and Tertre et al., 2006b)
$>SOH + Na^+ = >SONa + H^+$	-5.5	hexagonal-shaped
	-4.7	lath-shaped

Graphical Abstract

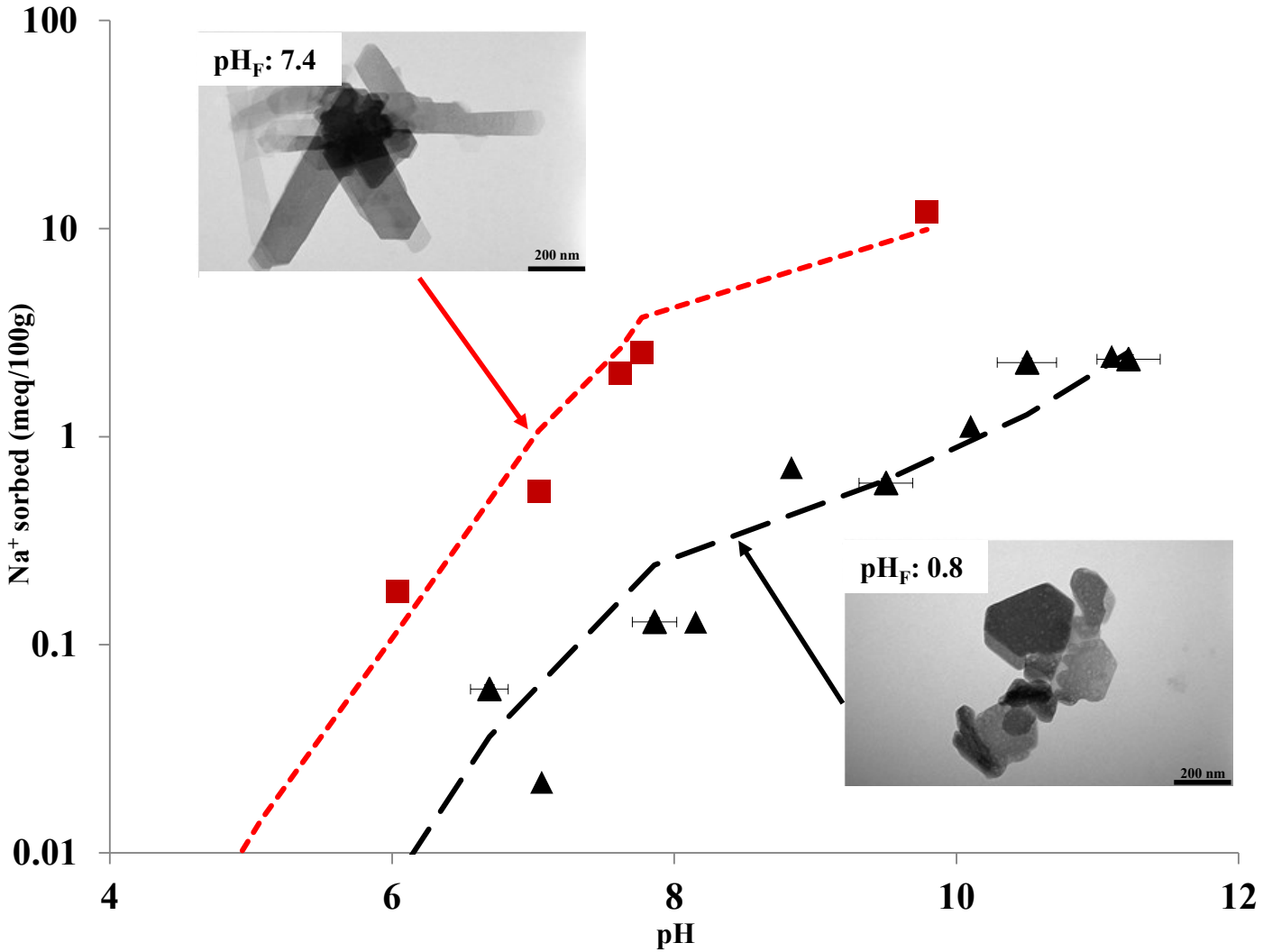

Highlights :

- Na^+/H^+ ion-exchange on kaolinites synthesized with a hydrothermal procedure.
- Synthetic kaolinites without permanent charge.
- Effect of the particle morphology on Na^+/H^+ selectivity coefficient.
- Sorption site densities for (010), (110) and (1-10) crystallographic faces.